Draft version December 16, 2008
Preprint typeset using LaTeX style emulateapj v. 03/07/07

INTERPRETATION OF THE EXTRAGALACTIC RADIO BACKGROUND

M. Seiffert[1], D. J. Fixsen[2,3], A. Kogut[2], S. M. Levin[1], M. Limon[4], P. M. Lubin[5], P. Mirel[2,6], J. Singal[7], T. Villela[8], E. Wollack[2], C. A. Wuensche[8]

Draft version December 16, 2008

ABSTRACT

We use absolutely calibrated data between 3 and 90 GHz from the 2006 flight of the ARCADE 2 instrument, along with previous measurements at other frequencies, to constrain models of extragalactic emission. Such emission is a combination of the Cosmic Microwave Background (CMB) monopole, Galactic foreground emission, the integrated contribution of radio emission from external galaxies, any spectral distortions present in the CMB, and any other extragalactic source. After removal of estimates of foreground emission from our own Galaxy, and the estimated contribution of external galaxies, we present fits to a combination of the flat-spectrum CMB and potential spectral distortions in the CMB. We find 2 σ upper limits to CMB spectral distortions of $\mu < 5.8 \times 10^{-5}$ and $|Y_{\rm ff}| < 6.2 \times 10^{-5}$. We also find a significant detection of a residual signal beyond that which can be explained by the CMB plus the integrated radio emission from galaxies estimated from existing surveys. After subtraction of an estimate of the contribution of discrete radio sources, this unexplained signal is consistent with extragalactic emission in the form of a power law with amplitude 1.06 ± 0.11 K at 1 GHz and a spectral index of -2.56 ± 0.04.

Subject headings: cosmology: cosmic microwave background — cosmology: observations

1. INTRODUCTION

The Cosmic Microwave Background (CMB) is currently our most precise window on the physics of the early universe. Measurements of the frequency spectrum of the CMB can rule out alternative cosmologies and place limits on physical processes that may distort the spectrum, including dark matter particle decay and reionization. Departures from a thermal blackbody spectrum are expected at a small level from a variety of mechanisms.

The *Cosmic Background Explorer* (*COBE*) satellite observed the spectrum of the CMB with the Far-Infrared Absolute Spectrophotometer (FIRAS) instrument (Mather et al. 1990) at wavelengths between 1 cm and 100 μm. FIRAS results reported by Fixsen et al. (1996), Mather et al. (1999) and Fixsen & Mather (2002) are consistent with a blackbody spectrum at a temperature of $T_{\rm CMB} = 2.725 \pm 0.001$ K.

Absolutely calibrated measurements of the CMB at longer wavelengths (lower frequency) than FIRAS have been performed with ground-based and balloon-borne experiments. Among the most sensitive of these measurements are those of Johnson and Wilkinson (1987), Levin et al. (1992), Bersanelli et al. (1994), Bersanelli et al. (1995), Staggs et al. (1996a), Staggs et al. (1996b), Raghunathan & Subrahmnayan (2000), Fixsen et al. (2004), Singal et al. (2006), and Zannoni et al. (2008).

[1] Jet Propulsion Laboratory, 4800 Oak Grove Drive, Pasadena, CA 91109; Michael.D.Seiffert@jpl.nasa.gov
[2] Code 665, Goddard Space Flight Center, Greenbelt, MD 20771
[3] University of Maryland
[4] Columbia Astrophysics Laboratory, 550W 120th St., Mail Code 5247, New York, NY 10027-6902
[5] University of California, Santa Barbara, CA
[6] Wyle Informations Systems
[7] Kavli Institute for Particle Astrophysics and Cosmology, SLAC National Accelerator Laboratory, Menlo Park, CA 94025
[8] Instituto Nacional de Pesquisas Espaciais, Divisão de Astrofísica, Caixa Postal 515, 12245-970 - São José dos Campos, SP, Brazil

The second generation of the Absolute Radiometer for Cosmic and Diffuse Emission (ARCADE 2) was conceived as a balloon-borne experiment to improve constraints on spectral distortions in the CMB, with particular emphasis on the 3 — 10 GHz frequency range. ARCADE 2 uses a unique, clear aperture instrument design with the bulk of the instrument operating at or near the temperature of the CMB. This minimizes the potential contribution to instrument systematics from warm, emissive optics. The instrument uses a set of microwave feed horns to compare the sky to a large, cryogenic blackbody calibration target. The results described here are from the second version of the instrument, described in detail by Singal et al. (2008). The sky measurements from the second flight of this instrument are described by Fixsen et al. (2008), which presents a detection of extragalactic emission consistent with a power law plus constant CMB temperature. The model of Galactic emission used in interpreting the ARCADE 2 data is described by Kogut et al. (2008).

In this paper, we use the combination of ARCADE 2 and other data sets to present a detection of 3 GHz emission in excess of that expected from the CMB and existing source counts of radio galaxies. The excess emission amplitude and spectral index described here differ from the extragalactic emission described by Fixsen et al. (2008). Here, we are concerned with the residual excess emission that cannot be explained from known classes of emission, and explicitly correct for the estimated contribution of discrete radio galaxies. We also use the combined data to place limits on spectral distortions to the CMB, and show that canonical spectral distortions cannot explain the excess emission.

This paper is organized as follows: Section 2 summarizes the estimates of isotropic, extragalactic emission at a variety of frequencies that we have used in our analysis. Section 3 examines the potential contribution of extragalactic point sources and their potential to affect our

conclusions. Section 4 presents our spectral fits to the data and our limits on spectral distortions of the CMB. Section 5 presents discussion of the results, including potential explanations for the source of the excess emission.

2. RESULTS FROM ARCADE 2 AND OTHER SURVEYS

For our analysis, we use the data from the 2006 flight of the ARCADE 2 instrument, from FIRAS, and from lower frequency ground-based surveys. FIRAS measures a high-precision difference between the sky and a calibrated reference target. The result is a set of values with tiny relative errors, and a larger, 1 mK calibration error common to all the data points. Table 1 summarizes the remaining data used in our analysis, which includes ARCADE 2, the 22 MHz survey of Roger et al. (1999), the 45 MHz survey of Maeda et al. (1999), the 408 MHz survey of Haslam et al. (1981), and the 1.42 GHz survey of Reich & Reich (1986). Kogut et al. (2008) describes the process of estimating the Galactic component from each of these data sets. the data in Table 1 is the resulting estimate of the residual, extragalactic, isotropic emission. The ARCADE 2 data in the 3 - 10 GHz range are shown in Figure 1; they lie significantly above the 2.725 K blackbody CMB determined by FIRAS at higher frequencies.

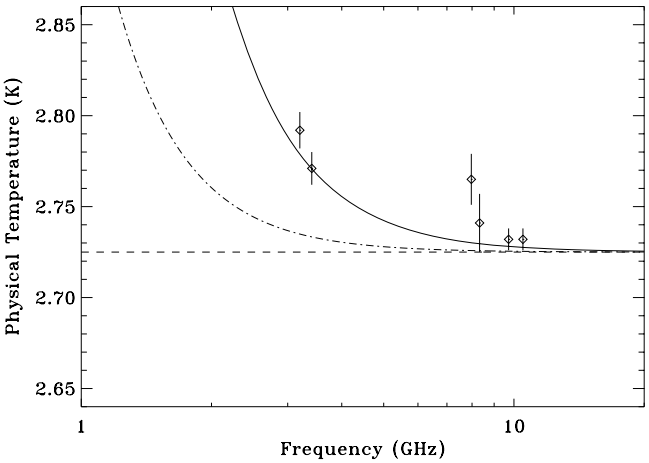

FIG. 1.— Detection of extragalactic radio emission by ARCADE 2 beyond the contribution of discrete radio sources and the expectation of 2.725 K blackbody radiation. Data points are the ARCADE 2 results from Fixsen et al. (2008), and have been corrected for Milky Way Galactic emission described by Kogut et al. (2008). The dashed curve is a constant 2.725 K blackbody, consistent with FIRAS measurements of the CMB. The dot dash curve is an estimate of the discrete radio source contribution from Gervasi et al. (2008a) model "Fit1" added to the 2.725 blackbody. The data points lie significantly above this dot dash curve, indicating our detection of unexplained, excess emission. The solid curve is the best fit of the combined data of Table 1 and FIRAS to a power law plus a constant CMB temperature.

In our analysis, we have excluded the 100-200 MHz results of Rogers & Bowman (2008). They find a minimum diffuse background of 237 K at 150 MHz, but their work does not provide an independent estimate of the Galactic contribution. We can, however, check for consistency by using the Galactic model described by Kogut et al. (2008) extrapolated to 150 MHz, where we find an approximately 60 K Galactic contribution to the diffuse background in the region of high Galactic latitude. Applying this correction, we find both the emission amplitude and spectral index are consistent with the fits we present in section 4.

We have similarly excluded the results reported by Bridle (1967) at 178 MHz (37 ± 8K) for an isotropic component. Here the agreement with the rest of the data is not as good, and is in mild disagreement with Rogers & Bowman (2008).

We have not included a number of other measurements, including the rocket-borne measurements of Gush, Halpern, & Wishnow (1990) and the ground-based and balloon-borne measurements cited earlier. The size of the uncertainties quoted in these measurements results in no significant contribution to the constraints on our model fits.

3. CONTRIBUTION OF SOURCES

The set of measurements in Table 1 do not have sufficient angular resolution to reject discrete radio sources. Instead, we must estimate the contribution of these sources through one of two ways: direct radio surveys designed to detect such sources, or measurements of the far-IR background which can trace the integrated emission of such sources through the correlation of the far-IR and radio emission. We examine these two methods in turn.

3.1. *Expectation from source counts*

The sky brightness temperature contributed by discrete sources can composed as the sum of two parts: the source population that has been characterized by existing surveys and the contribution of sources below the flux limit of existing surveys. We write this as:

$$T = T(S > S_{\rm limit}) + \frac{\lambda^2}{2k_{\rm B}} \int_{S_{\rm min}}^{S_{\rm limit}} \frac{dN}{dS} S dS, \qquad (1)$$

where $T(S > S_{\rm limit})$ is contribution from sources with a flux S greater than the survey limit $S_{\rm limit}$. The wavelength of observation is λ and $k_{\rm B}$ is the Boltzmann constant. We characterize sources below the survey limit with their differential number counts, dN/dS, and assume that there is a lower limit cutoff to the source population at a flux of $S_{\rm min}$. Radio source count surveys reveal a faint source population with differential number counts proportional to a power law

$$\frac{dN}{dS} = S^{-\gamma}. \qquad (2)$$

An index γ of 2.5 corresponds to a static, Euclidean universe with uniform filling of sources, whereas faint radio surveys find γ in the range of 2.0 to 2.3. Such source counts can not extend to arbitrarily low fluxes, or the total contribution would diverge. A realistic distribution of sources, of course, would not have a sharp cutoff at $S_{\rm min}$. In practice, we can characterize $S_{\rm min}$ as the flux below which the index γ falls below 2, as there will be negligible additional contribution to the integral below this limit.

Deep surveys of radio sources have been performed at a number of frequencies. Particularly useful are the

TABLE 1
Measurements of Extragalactic Radio Emission

Frequency (GHz)	Extragalactic[a] Temperature (K)	Error (K)	Radio Sources[b]	Error[c]	Residual Emission[d]	Error[e]
0.022	21200[f]	5125[f]	7090	709	14100	5175
0.045	4355[g]	520[g]	1020	102	3334	530
0.408	16.24[h]	3.40[h]	2.61	0.26	13.6	3.41
1.42	3.213[j]	0.53[j]	0.089	0.009	3.124	0.53
3.20	2.792[k]	0.010[k]	0.010	0.001	2.782	0.010
3.41	2.771[k]	0.009[k]	0.008	< 0.001	2.763	0.009
7.97	2.765[k]	0.014[k]	< 0.001	< 0.001	2.764	0.014
8.33	2.741[k]	0.016[k]	< 0.001	< 0.001	2.740	0.016
9.72	2.732[k]	0.006[k]	< 0.001	< 0.001	2.732	0.006
10.49	2.732[k]	0.006[k]	< 0.001	< 0.001	2.732	0.006
29.5	2.529[k]	0.155[k]	< 0.001	< 0.001	2.529	0.155
31	2.573[k]	0.076[k]	< 0.001	< 0.001	2.573	0.076
90	2.706[k]	0.019[k]	< 0.001	< 0.001	2.706	0.019

[a] This is the monopole temperature with the Milky Way Galactic contribution removed as by Kogut et al. (2008)
[b] Estimate of extragalactic discrete radio source contribution from Gervasi et al. (2008a) model "Fit1".
[c] We have adopted a 10% fractional error for the Gervasi et al. (2008a) "Fit1" model (see text).
[d] Residual extragalactic emission after subtraction of radio source
[e] Error in residual extragalactic emission after subtraction of radio source
[f] Data from Roger et al. (1999) corrected for Galactic emission with the model described by Kogut et al. (2008)
[g] Data from Maeda et al. (1999) corrected for Galactic emission with the model described by Kogut et al. (2008)
[h] Data from Haslam et al. (1981) corrected for Galactic emission with the model described by Kogut et al. (2008)
[j] Data from Reich & Reich (1986) corrected for Galactic emission with the model described by Kogut et al. (2008)
[k] ARCADE 2 Fixsen et al. (2008)

surveys at 1.4 and 8.4 GHz with the Very Large Array (VLA). Fomalont et al (2002) reports the results of an 8.4 GHz survey with a survey limit of 7.5μJy and finds a faint-end index to the number counts of $\gamma = 2.11 \pm 0.13$. Windhorst et al (1993) argue that the sources in the nJy flux range are dominated by ordinary spiral galaxies, which produces a natural lower limit of 30 nJy; below this limit there are insufficient galaxies.

Figure 2 shows a range of estimates for the contribution of discrete sources to the ARCADE 2 3.20 GHz measurement. We have calculated the expected contribution to the extragalactic sky temperature using the results of Fomalont et al (2002) and varying the faint end index, and plotting as a function of $S_{\rm min}$. We have scaled the temperature from 8.4 to 3.2 GHz using a frequency spectral index of -2.75. This spectral index is characteristic of starburst and normal spiral galaxies with synchrotron emission, though at 8.4 GHz there could be some contribution from flat spectrum sources such as AGN. The sources fainter than 35 μJy described by Fomalont et al (2002) have a spectral index distribution that peaks at -2.75. From this analysis, we conclude that the contribution is likely in the range of 5 to 10 mK at 3.20 GHz.

It is interesting to consider to what extremes one would need to take the number counts in this analysis to account for the measured 58 mK excess at 3.20 GHz. Using an index of $\gamma = 2.5$ and extrapolating the number counts from Fomalont et al (2002), we find that we would need to extend the lower flux limit to 0.3 nJy, which would result in a source density of $\sim 8 \times 10^5$ per square arcmin. This extreme scenario is not a plausible distribution of ordinary galaxies. We also note that the normalization of the differential number counts in the 8.4 GHz survey is sufficiently accurate to not contribute a significant source of error to this analysis.

We have focused on the 8.4 GHz survey results, as these measurements are amenable to extrapolation to fainter fluxes and to the ARCADE 2 frequencies. Our results, however, do not depend on the results from a radio survey at one frequency. Gervasi et al. (2008a) describe a more comprehensive analysis of the potential contribution of unresolved extragalactic radio sources by examining data from a wide variety of radio surveys, and fitting an em-

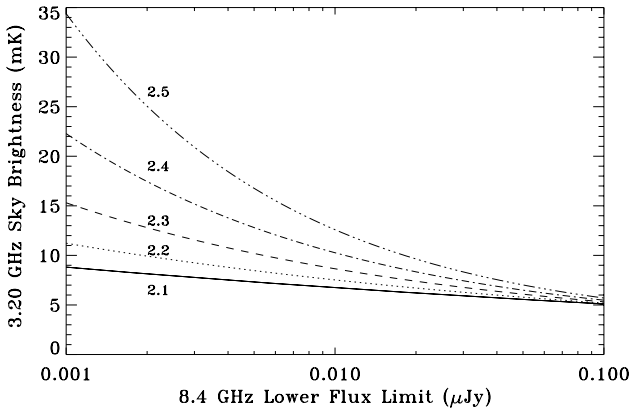

Fig. 2.— Estimated contribution of extragalactic source counts to the sky brightness at 3.20 GHz, versus the assumed faint end cutoff of 8.4 GHz source counts. The sky brightness is first calculated at 8.4 GHz from the sum of the existing source population greater than 7.5 μJy (Fomalont et al 2002) and the contribution of fainter sources assuming a continuation of the differential number counts with a power law index of 2.1 (solid curve), 2.2 (dotted curve), 2.3 (dashed curve), 2.4 (dash dot curve), and 2.5 (dash dot dot curve). The contribution is scaled to the ARCADE 3.20 GHz channel with a frequency index of -2.75, as is typical of sources in faint radio surveys. The measured index of differential number counts at the faint end of the 8.4 GHz survey is $\gamma = 2.11 \pm 0.13$.

pirical, two-population model to the survey data at each frequency. Their combined result for extragalactic radio source brightness versus frequency is described by a single power law model, "Fit1", with amplitude 0.88 K at 0.61 GHz, and a power law index of -2.707. This model is also shown in Figure 1, indicating again that this contribution is insufficient to explain the ARCADE 2 results. The brightness temperature values of this model, evaluated at the frequencies used in our analysis, appear in Table 1. Because the sample size and brightness limits of the radio surveys vary with frequency, the error in their estimate also varies with frequency. These frequencies are not identical to the frequencies measured by ARCADE 2. For Table 1, we adopt a fractional error estimate of 10% independent of frequency, which we believe is a conservative estimate of the error in the Gervasi et al. (2008a) modeling. These estimates for the contribution of extragalactic sources are consistent with the analysis described above.

It also is interesting to consider whether the existing surveys have missed significant flux from the sources. The low frequency faint source observations are primarily interferometric and have the possibility of overresolving the source and missing flux in extended low surface brightness emission. Henkel & Partridge (2005) consider the evidence for this and conclude that 20% may be an upper limit to this effect for mJy flux levels at 8.5 GHz. Fomalont et al. (2006) suggests that at 1.4 GHz only a few percent of sources are larger than 4 arc seconds and that other reports of a larger figure in other surveys are actually confusion of multiple disparate sources. Garrett et al. (2000) compare their 1.4 GHz survey conducted using the Westerbork Synthesis Radio Telescope and its larger, 15 arcsec effective beam with previous VLA measurements of the same region with a similar noise level. Of a total of 85 sources in their survey, they find 22 not apparent in the previous VLA survey. Some of these 22 likely correspond to the combined flux of multiple sources that were resolved by the VLA measurements. At least 2 sources, however, appear to be relatively nearby discrete sources with emission from a large enough region to have been resolved out by the VLA measurements. We conclude from these studies that it seems unlikely that sufficient flux has been missed in surveys of known objects to explain our residual emission.

Another method to examine the possibility of extended low surface brightness emission in extragalactic sources is radio observations of the halos of nearby edge on spirals. Irwin, English, & Sorathia (1999) and Irwin, Saikia, & English (2000) report results of VLA surveys for radio emission from nearby edge-on spirals. These studies can elucidate the connection between the star formation processes that drive the far-IR background, and the supernova processes that drive radio emission, but do not provide evidence that large amounts of radio flux are missed in surveys of more distant sources.

3.2. *Connection with Far-IR Background*

The cosmic far-IR background has been detected at a level of approximately $10 - 20\,\mathrm{nW\,m^{-2}\,sr^{-1}}$ with FIRAS and DIRBE (Puget et al. 1996; Fixsen et al. 1998; Hauser et al. 1998). We can use the universal radio to far-IR correlation in star-forming galaxies (Condon 1992) to estimate the expected extragalactic radio background that can be attributed to galaxies contributing to the cosmic far-IR background. Haarsma & Partridge (2000) and Dwek & Barker (2002) specifically address this prospect. The conclusion of these studies is that the far-IR measurements are consistent with the existing surveys of radio galaxies described earlier. For example, the radio brightness temperature of 18 K at 178 MHz predicted by Dwek & Barker (2002) is within 1 σ of the radio galaxy contribution modeled by Gervasi et al. (2008a). This emission is insufficient to account for the excess detected by ARCADE 2.

There is no obvious way around this limit by considering departures from the far-IR radio correlation associated with faintness or redshift. Garn & Alexander (2008) stack IR-selected galaxies and data from faint radio surveys and find there is no evidence for a change in the far-IR to radio correlation with fainter galaxies. Similarly, there does not appear to be evidence for a change in the far-IR to radio correlation with redshift (Chapman 2005; Frayer et al. 2006).

There is some room for breaking the far-IR to radio correlation; the physical processes of far-IR emission from dust heated by star formation and radio emission driven by supernovae are related but differ in timescale (see, e.g., Murphy et al. 2008). There does not appear, however, to be a case for a sufficient difference in timescale to account for our measurements in known populations of galaxies.

4. FIT OF MODEL SPECTRUM

Here we fit a model spectrum to the combined data set of the residual emission column of Table 1 and the higher frequency results from FIRAS. The form of the fitting function is:

$$T(\nu) = T_0 + A\,(\nu/1\ \mathrm{GHz})^{\beta} + \Delta T(\nu), \qquad (3)$$

where T_0 is the CMB baseline temperature, A is the power law amplitude at 1 GHz, β is the power law index, ν is frequency, and $\Delta T(\nu)$ is a CMB spectral distortion. Data are converted (where necessary) to units of antenna temperature before fitting using:

$$T_{\mathrm{Ant}} = \frac{h\nu/k}{e^{h\nu/kT_{\mathrm{Phys}}} - 1}, \qquad (4)$$

where h is Planck's constant, k is Boltzmann's constant, T_{Ant} is antenna temperature, and T_{Phys} is the physical temperature. We use a Levenberg-Marquardt nonlinear least-squares minimization for the fitting procedure (Marquardt 1963). We have allowed for the 1 mK relative calibration uncertainty between the FIRAS temperature scale and the other measurements in determining the size of the errors on the fit parameters. This was accomplished by adding or subtracting 1 mK to the FIRAS measurements and noting the change in the parameter value. This change was then added in quadrature to the error derived without allowing the relative calibration error. In most cases this makes a only very small difference. The exception is T_{CMB}, where we recover the expected 1 mK error. The parameters for the fits described in this section are summarized in Table 2.

4.1. *Power-Law Plus CMB*

Figure 1 shows that there is clear excess emission detected by ARCADE 2 in the 3 GHz channels compared

to what is expected from the CMB plus the contribution of extragalactic radio sources. The unexplained residual emission is consistent with a power law with amplitude 1.06 ± 0.11 K at 1 GHz, with a spectral index of $\beta = -2.56 \pm 0.04$.

We have also experimented with inflating the assumed errors for the removal of extragalactic discrete sources. As noted in Section 3.1, we have assumed a fractional error of 10%, independent of frequency, for the discrete source contribution model. Inflating this error to 50% fractional error makes much less than a 1 σ change in the values of our power law fit parameters above, and only a small ($\sim 10\%$) increase in the quoted errors in the fit parameters. This is because the error in the removal of the discrete sources is smaller than the other errors in the low frequency measurements, as can be seen by inspection of Table 1.

4.2. *Free-Free Distortions*

Free-free distortions to the CMB spectrum can arise from energy released at lower redshifts (Bartlett & Stebbins 1991; Gnedin & Ostriker 1997; Oh 1999), and can be characterized by

$$\Delta T_{\rm ff}(\nu) = T_0 \frac{Y_{\rm ff}}{x^2}, \tag{5}$$

where $Y_{\rm ff}$ is the optical depth to free-free emission, T_0 is the undistorted CMB temperature, x is the dimensionless frequency $h\nu/kT_0$, and ΔT is apparent temperature distortion.

A lower limit can be placed on the optical depth to free-free emission from late time effects of $Y_{\rm ff} > 8 \times 10^{-8}$ (Haiman & Loeb 1997). The current upper limit of $Y_{\rm ff} < 1.9 \times 10^{-5}$ comes from combining data from FIRAS and previous ground-based CMB spectrum measurements (Bersanelli et al. 1994).

We have performed a four component fit to the data to assess whether there is evidence to support a free-free spectral distortion to the CMB, compared to the three parameter fit described in the previous section. The four fit components consist of a constant CMB temperature, a power law amplitude, a power law index, and a free-free amplitude. The fit parameters are presented in Table 2. The addition of the free-free amplitude does not improve the reduced χ^2 of the fit compared to the fit presented in Figure 1 and is therefore not justified by the data.

We have also examined a two parameter fit consisting of a constant CMB component and free-free distortion component; the parameters are shown in Table 2. This fit produces a significantly worse reduced χ^2, and is therefore not consistent with the source of the unexplained emission.

The 2σ limits on the free-free amplitude at 1 GHz derived from our four parameter fit are $-0.44{\rm K} < \Delta T_{Y_{\rm ff}} < 0.52{\rm K}$. This corresponds to an upper limit on the free-free optical depth of

$$|Y_{\rm ff}| < 6.2 \times 10^{-5} \tag{6}$$

This limit is less constraining than those reported by Bersanelli et al. (1994) and Gervasi et al. (2008b). This is the result of the additional degrees of freedom allowed by our four parameter fit. As described above, the four parameter fit is a better description of the data than the CMB plus free-free distortion fits performed by Bersanelli et al. (1994) and Gervasi et al. (2008b). We conclude that the tighter constraints offered by those studies are likely too optimistic.

It is interesting to consider how future measurements might improve the $Y_{\rm ff}$ limit. We have used the existing fits and asked how much tighter the limit becomes if an additional measurement of some fixed fractional accuracy is added to the data set. We have run this test as a function of frequency; the frequency range with the greatest effect is between 0.3 and 3.0 GHz, where a factor of several tighter constraint is potentially achievable. The results are shown in Figure 3, where we have plotted the size of the 2 σ errors on $Y_{\rm ff}$ as a function of the frequency of the additional measurement. We have assumed that the measurement point falls precisely on the existing fit. Better fractional error results in tighter constraints on $Y_{\rm ff}$. We have also considered the impact of repeating this test with additional measurements at 3, 5, 8, 10, 30, and 90 GHz with 0.002 K precision, as might be obtained with a future flight of ARCADE. Such a measurement would enhance the power of future lower frequency measurements to constrain $Y_{\rm ff}$.

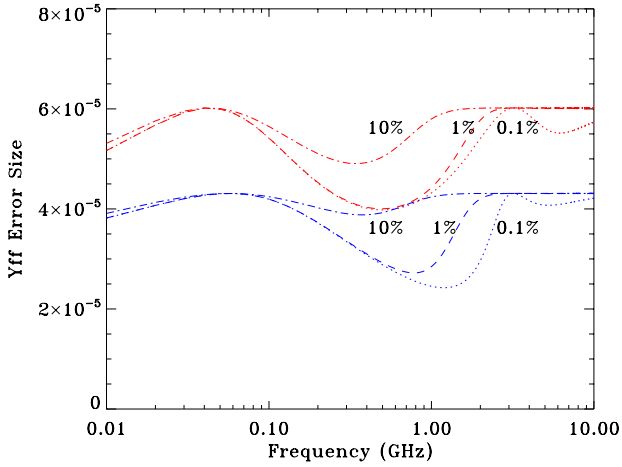

FIG. 3.— Improvement of limit on $Y_{\rm ff}$ obtainable with future measurements. Shown are the sizes of the 2 σ errors on $Y_{\rm ff}$ (red curves) that would result from an additional measurement at a frequency shown on the x-axis, with a precision of 0.1% (dotted curve), 1% (dashed curve), or 10% (dot dashed curve). The blue curves repeat this test under the assumption that there are additional measurements at 3, 5, 8, 10, 30, and 90 GHz with 0.002 K precision. The additional measurement is assumed to be centered on the value of the existing fit.

4.3. *Chemical Potential (μ) Distortions*

As we have discussed, energy release early in the universe can distort the spectrum of the CMB. Energy injection after a redshift of $\sim 10^6$ no longer results in a planckian spectrum, but instead forms a spectrum with a Bose-Einstein photon occupation number (Sunyaev & Zeldovich 1970):

$$\eta(x) = \frac{1}{e^{x+\mu(x)} - 1}, \tag{7}$$

where $x \equiv h\nu/kT$ is the dimensionless frequency, and $\mu(x)$ is a frequency-dependent chemical potential. A series of papers (Danese & De Zotti 1980; Burigana,

TABLE 2
Spectral Fits to Combined ARCADE 2, FIRAS, Radio Survey Data

Parameter	Power Law Fit	Power Law + $Y_{\rm ff}$	$Y_{\rm ff}$ Only	Power Law + μ Distortion
$T_{\rm CMB}$ [a]	2.725 ± 0.001	2.725 ± 0.001	2.725 ± 0.001	2.725 ± 0.001
Power Law Amplitude [b]	1.06 ± 0.11	1.00 ± 0.37	···	1.05 ± 0.11
Power Law Index	-2.56 ± 0.04	-2.58 ± 0.11	···	$-2.56 \pm .05$
Free-Free Amplitude [c]	···	0.04 ± 0.24	0.54 ± 0.07	···
μ Amplitude	···	···	···	$(-0.73 \pm 3.3) \times 10^{-5}$
Degrees of Freedom	53	52	54	52
χ^2	60.8	60.8	107.1	60.8
Reduced χ^2	1.15	1.17	1.98	1.17

[a] The best fit thermodynamic temperature of the CMB in K.
[b] The fit amplitude of a power law component in K (antenna temperature) at 1 GHz.
[c] The fit amplitude of $\Delta T_{Y_{\rm ff}}$ in K (antenna temperature) at 1 GHz.

Danese, & De Zotti 1991a,a, 1995) has investigated in detail the shape of the resulting spectral distortions after inclusion of free-free processes which act at the low frequency end. The shape of the distortion depends on the range of redshift over which such energy injection takes place. We have used their analytic description of such distortions to the CMB to provide a functional form to fit the data in Table 1. A necessary ingredient is the baryon density, for which we adopt a value of $\Omega_b h^2 = 0.02265$, from the 5-year WMAP data, including constraints from Baryon Acoustic Oscillation and Supernova measurements as described by Hinshaw et al. (2008).

In addition to the μ distortion, we have included a power law amplitude and index to the fit parameters. Figure 4 shows the result of the fit as well as the residuals. The addition of the μ distortion as a free parameter does not improve the reduced χ^2. The 2σ upper limit on μ is

$$\mu < 5.8 \times 10^{-5}. \quad (8)$$

This limit is an improvement on the previous limit of 9×10^{-5} set using FIRAS (Fixsen et al. 1996). Although it is numerically similar to the limit reported recently by Gervasi et al. (2008b), we believe it to be a more robust limit because we have allowed additional free parameters in our fit.

5. DISCUSSION

We have presented evidence for isotropic radio emission detected by ARCADE 2 beyond what can be explained by Galactic emission and the unresolved emission from the known population of discrete sources. The excess emission is consistent with a power law, with an index of -2.56, which is significantly flatter that what might be expected from an unidentified population of faint, diffuse, steep spectrum (index ~ -2.7) radio sources associated with star-forming galaxies. We have also examined and placed limits on two classes of spectral distortions to the CMB. Such distortions are not supported by the data and cannot explain the excess emission, as is illustrated graphically in Figure 4.

It is possible to imagine that an unknown population of discrete sources exist below the flux limit of existing surveys. We argue earlier that these cannot be a simple extension of the source counts of star-forming galaxies. As a toy model, we consider a population of sources distributed with a delta function in flux a factor of 10 fainter than the 8.4 GHz survey limit of Fomalont et al (2002). At a flux of 0.75 μJy, it would take over 1100 such sources per square arcmin to produce the unexplained emission we see at 3.20 GHz, assuming a frequency index of -2.56. This source density is more than two orders of magnitude higher than expected from extrapolation to the same flux limit of the known source population. It is, however, only modestly greater than the surface density of objects revealed in the faintest optical surveys, e.g., the Hubble Ultra Deep Field (Beckwith et al. 2006). The unexplained emission might result from an early population of non-thermal emission from low-luminosity AGN; such a source would evade the constraint implied by the far-IR measurements.

We believe our result to be robust to several potential sources of error. Underestimating the level of Galactic emission is a potential contaminant. As described by Kogut et al. (2008), however, the expected contribution of the area around the North Galactic Pole is only $\sim$ 0.5 K at 1 GHz, with relatively tight errors. Further, the Galactic emission is estimated with two independent methods along several lines of sight.

Relativistic electrons trapped in the Earths magnetic field emit synchrotron radiation (Dyce & Nakada 1959). This emission is polarized and anisotropic, however, with intensity peaking near the Earths magnetic equator and falling to zero at the poles. Further, it is measured to be less than 3 K at 30 MHz and expected to be much less than 1 mK at 3 GHz (Ochs et al. 1963; Peterson & Hower 1963). It therefore is unlikely to be the source of the unexplained emission.

Correcting for instrumental systematic errors in measurements such as ARCADE 2 is always a primary concern. We emphasize that we detect unexplained emission at 3 GHz with the ARCADE 2 data, but the result is also independently detected by a combination of low frequency data and FIRAS. As described by Fixsen et al. (2008), the extragalactic emission is detected above 3σ with any two of the three data subsets: 1) FIRAS and low frequency radio data, 2) ARCADE 2 and low frequency radio data, and 3) ARCADE 2 and FIRAS. The result is therefore robust to problems in any one measurement.

We conclude that the three most important sources of error, Galactic emission, instrumental systematic errors, and radio emission from the faint end of the distribution of known sources, are unlikely to be sufficient to explain the excess emission presented here.

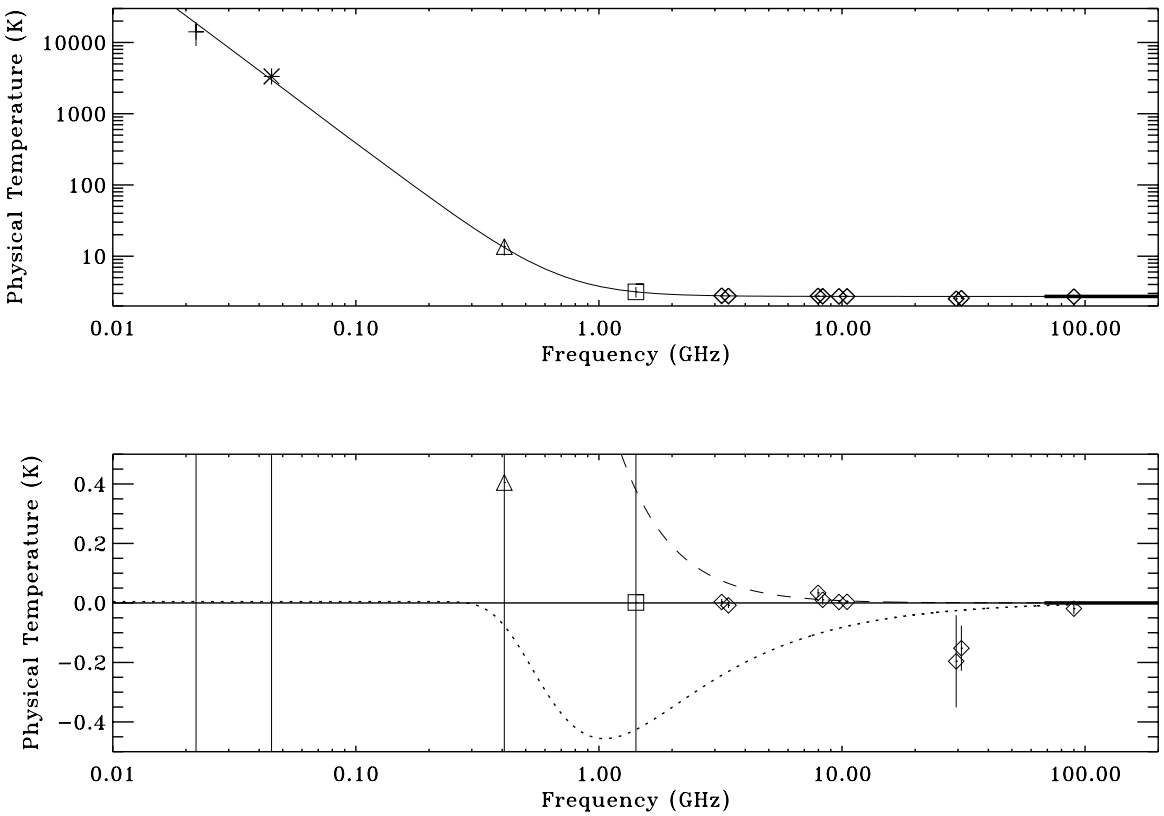

FIG. 4.— Fit of ARCADE 2 data, FIRAS data, and data from low frequency radio surveys. The upper plot shows (solid line) a fit with three components: a frequency independent CMB contribution, a power law amplitude, and a power law index. The lower plot shows the fit residuals. The dotted line shows the expected shape of a μ distortion. The amplitude of the plotted distortion is 100 times the 2σ upper limit allowed by the fit. The dashed line shows the shape of a $Y_{\rm ff}$ distortion with an amplitude equal to the 2σ upper limit. The addition of either a μ distortion or a $Y_{\rm ff}$ distortion as a free parameter is not supported by the data. Data points are from Roger et al. (1999) (cross), Maeda et al. (1999) (asterisk), Haslam et al. (1981) (triangle), Reich & Reich (1986) (square), ARCADE 2 (diamonds), and FIRAS (heavy line), corrected for Galactic emission and an estimate of extragalactic radio sources, as shown in Table 1.

It is a pleasure to thank the staff of the Columbia Scientific Balloon Facility for their support of ARCADE 2. We thank the undergraduate students whose work helped make ARCADE 2 possible: Adam Bushmaker, Jane Cornett, Sarah Fixsen, Luke Lowe, and Alexander Rischard. ARCADE 2 was supported by the National Aeronautics and Space Administration suborbital program. T.V. acknowledges support from CNPq grants 466184/00-0, 305219-2004-9, and 303637/2007-2-FA, and the technical support from Luiz Reitano. C.A.W. acknowledges support from CNPq grant 307433/2004-8-FA. The research described in this paper was performed in part at the Jet Propulsion Laboratory, California Institute of Technology, under a contract with the National Aeronautics and Space Administration.

REFERENCES

Beckwith, S.V. et al., 2006, AJ, 132, 1729
Bersanelli, M., Bensadoun, M., de Amici, G., Levin, S., Limon, M., Smoot, G. F., & Vinje, W. 1994, ApJ, 424, 517
Bersanelli, M., Smoot, G. F., Bensadoun, M., de Amici, G., Limon, M., & Levin, S. 1995, Astrophys. Lett. Commun., 32, 7
Bridle, A.H., 1967, MNRAS, 136, 219
Burigana, De Zotti, Danese, A&A, 303, 323, 1995
Burigana, Danese, De Zotti A&A, 246, 49, 1991
Burigana, Danese, De Zotti ApJ, 379, 1, 1991
Bartlett & Stebbins, ApJ, 317, 8, 1991
Chapman, S.C., Blain, A.W., Smail, I., & Ivison, R.J. 2005, ApJ, 622, 772
Danese & De Zotti A&A, 84, 364, 1980
Dwek & Barker, ApJ, 575, 7, 2002
Dyce, R.B. & Nakada, M.P. 1959, JGR, 64, 1163
Fixsen, D.J, et al., 1996, ApJ, 473, 576
Fixsen, D.J, et al. 1998, ApJ, 508, 123
Fixsen, D.J, & Mather, J.C., ApJ, 2002, 581, 817
Fixen, D. J., et al. 2004, ApJ, 612, 86
Fixsen et al., ApJ, submitted, 2008
Fomalont et al, AJ, 123, 2402, 2002
Fomalont et al, ApJS, 167, 103, 2006
Frayer, D.T., et al. 2006, AJ, 131, 250
Garn, T., & Alexander, P., 2008, MNRAS, accepted
Garrett, M.A., de Bruyn, A.G., Giroletti, M., Baan, W.A., & Schilizzi, R.T., 2000, A&A, 361, L41
Gervasi, M. et al., ApJ, 2008, 682, 223
Gervasi, M. et al., ApJ, 2008, 688, 24
Gnedin & Ostriker, ApJ, 486, 581, 1997
Gush, H.P., Halpern, M., & Wishnow, E.H., 1990, PRL, 65, 537
Haarsma & Partridge, ApJ, 544, 641, 2000
Haiman & Loeb, ApJ, 483, 21, 1997
Haslam, C.G.T., et al., 1981, A&A, 100, 209
Hauser, M.G., et al. 1998, ApJ, 508, 25
Henkel & Partridge, ApJ, 635, 950, 2005
Hinshaw, G. et al., 2008, ApJ, accepted.
Irwin, J.A., English, J., & Sorathia, B. 1999, AJ, 117, 2102
Irwin, J.A., Saikia, D.J., & English, J. 2000, AJ, 119, 1592

Johnson, D. & Wilkinson, D., 1987, ApJ, 313, L1
Kogut et al., ApJ submitted, 2008
Levin, S., Bensadoun, M., Bersanelli, M., de Amici, G., Kogut, A., Limon, M., & Smoot, G. 1992, ApJ, 396, 3
Maeda, K., Alvarez, H., Aparici, J., May, J., and Reich, P., 1999, A&AS, 140, 145
Marquardt, D.W., Journal of the Society for Industrial and Applied Mathematics, 11, 431, 1967
Mather, J.C. et al., ApJ, 1999, 512, 511
Mather, J.C. et al., ApJ, 1990, 354, L37
Murphy, Helou, Kenney, Armus, & Braun, ApJ, 678, 828, 2008
Ochs,G.R., Farley, D.T. Jr., & Bowles, K.L. 1963, JGR, 68, 701
Oh, ApJ, 527, 16, 1999
Peterson,A.M. & Hower,G.L. 1963 JGR, 68, 723
Puget, J.-L. et al. 1996 A&A 308, L5
Raghunathan, A., & Subrahmnayan, R. 2000, J. Astrophys. Astron., 20, 1
Reich, P. and Reich, W., 1986, A&AS, 63, 205
Roger, R.S., Costain, C.H., Landecker, T.L., and Swerdlyk, C.M., 1999, A&AS, 137, 7
Rogers, Alan E. & Bowman, Judd D., 2008, AJ, 136, 641
Singal, J., et al. 2006, ApJ, 653, 835
Singal et al., ApJ submitted, 2008
Staggs, S., Jarosik, N. C., Meyer, S. S., & Wilkinson, D. T. 1996a, ApJ, 473, L1
Staggs, S., Jarosik, N. C., Wilkinson, D. T., & Wollack, E. J. 1996b, ApJ, 458, 407
Sunyaev, R.A. & Zeldovich,Ya.B., 1970, Ap&SS, 7, 20
Windhorst et al, ApJ, 405, 498, 1993
Zannoni, M., Tartari, A., Gervasi, M., De Lucia, A., Passerini, A., Cavaliere, F., Boella, G., & Sironi, G. 2008, ApJ, 688, 12